Hindawi Publishing Corporation
International Journal of Antennas and Propagation
Volume 2016, Article ID 6367205, 6 pages
http://dx.doi.org/10.1155/2016/6367205

Research Article

Efficient Computation of Wideband RCS Using Singular Value Decomposition Enhanced Improved Ultrawideband Characteristic Basis Function Method

Wen-yan Nie[1] and Zhong-gen Wang[2]

[1]*College of Mechanical and Electrical Engineering, Huainan Normal University, Huainan, Anhui 232001, China*
[2]*College of Electrical and Information Engineering, Anhui University of Science and Technology, Huainan, Anhui 232001, China*

Correspondence should be addressed to Zhong-gen Wang; zgwang@ahu.edu.cn

Received 26 August 2016; Accepted 17 November 2016

Academic Editor: Ding-Bing Lin

The singular value decomposition (SVD) enhanced improved ultrawideband characteristic basis function method (IUCBFM) is proposed to efficiently analyze the wideband scattering problems. In the conventional IUCBFM, the SVD is only applied to reduce the linear dependency among the characteristic basis functions (CBFs) due to the overestimation of incident plane waves. However, the increase in the size of the targets under analysis will require a large number of incident plane waves and it will become very time-consuming to solve such numbers of the matrix equation. In this paper, the excitation matrix is compressed by using the SVD in order to reduce both the number of matrix equation solutions and the number of CBFs compared with the traditional IUCBFM. Furthermore, the dimensions of the reduced matrix and the reduced matrix filling time are significantly reduced. Numerical results demonstrate that the proposed method is accurate and efficient.

1. Introduction

System response over a wide frequency band is required in many applications, such as modern radar target recognition, microwave remote sensing, and microwave imaging. The method of moments (MoM) [1] is one of the most popular numerical methods used for radar cross section (RCS) prediction, but it places a heavy burden on memory and solving time while dealing with electrically large problems. A number of different fast solution methods have been proposed to circumvent this problem such as the fast multipole method (FMM) [2], the multilevel fast multipole method (MLFMM) [3, 4], the adaptive integration method (AIM) [5], the adaptive cross approximation (ACA) algorithm [6], and the characteristic basis function method (CBFM) [7, 8]. Many electromagnetic applications require the solution of the radiation from an antenna or the scattering problem over a wide frequency band rather than at a single frequency point. However, the solution of the problem using either the conventional CBFM or other abovementioned fast solution methods requires the calculations to be executed at each frequency point. This creates a heavy burden on CPU time, especially for analyzing electrically large objects. Existing methods for computing wideband RCS are based on interpolating the MoM matrix [9] or utilizing the frequency and the frequency derivative data [10] with reduced frequency samples. However, the CPU time for these methods may become prohibitively high when the electrical size of the body is large. Hence, in [11], an ultrawideband characteristic basis function method (UCBFM) has been proposed to analyze the wideband electromagnetic scattering problems. The ultrawideband characteristic basis functions (UCBFs) constructed at the highest frequency point in the range of interest can be reused at lower frequency points without repeating the time-consuming process of generating the characteristic basis functions (CBFs). However, as indicated in [11], the RCS errors calculated by the UCBFs are usually large at lower frequency points. The reason for this is that the procedures are employed at the lower frequency points using the discretization carried out at the highest frequency which

resulted in an increased number of conditions while calculating the impedance matrix. Moreover, these UCBFs have been constructed at the highest frequency point, and their number is higher than necessary for lower frequency points. This leads to a reduced matrix whose dimensions are larger than required. The number of unnecessary UCBFs increases with the decrease in frequency. As a result, the computational time for the calculation and the solution of the reduced matrix at lower frequency points will be much higher than needed. To mitigate these problems, some improved methods have been presented. In [12], the construction of the UCBFs has been improved by fully considering the mutual coupling effects among the subblocks to obtain the secondary level CBFs (SCBFs), such that the improved UCBFs (IUCBFs) contain more current information and improve the calculation accuracy at lower frequency points. In [13], an adaptive IUCBFs construction method has been proposed and the adaptive IUCBFs have been obtained at the highest frequency point in each subband which leads to a smaller number of IUCBFs and significant reduction of solver time at lower frequency band. In [14], the unnecessary UCBFs have been removed from the basis set as the frequency is decreased. However, in the generation step of the IUCBFs in [12–14], the choice of the number of incident plane waves (PWs) is typically made empirically and the redundant PWs are usually chosen which increases the solving time of the CBFs. To mitigate this problem, singular value decomposition (SVD) is adapted to enhance the efficiency of the CBFs generation in this paper. In the new proposed scheme for generating the CBFs, fewer matrix equation solutions are required and the number of the CBFs is reduced. Furthermore, the dimensions of the reduced matrix and the reduced matrix filling time are significantly reduced.

The remainder of the paper is organized as follows. In Section 2, the conventional IUCBFM is briefly described. Section 3 describes the use of the SVD to efficiently speed up the CBFs generation by reducing the number of PWs. In Section 4, some numerical results are presented, while conclusions are drawn in Section 5.

2. Improved Ultrawideband Characteristic Basis Function Method

The IUCBFM [12] begins by dividing the object into M blocks. Then, it establishes a model at the highest frequency point. Multiangle PWs are set to irradiate each block. Suppose N_θ and N_ϕ represent the numbers of PWs in directions of θ and ϕ, respectively, and in total $N_{\text{pws}} = 2N_\theta N_\phi$ (two polarization modes are considered), noted as $\mathbf{E}_{ii}^{N_{\text{pws}}}$. To obtain the PCBFs of each block, one must solve the following system:

$$\mathbf{Z}_{ii} \cdot \mathbf{J}_{ii}^{\text{CBF}} = \mathbf{E}_{ii}^{N_{\text{pws}}}, \tag{1}$$

where $\mathbf{Z}_{ii}$ is an $N_i \times N_i$ self-impedance matrix of block i, for $i = 1, 2, \ldots, M$; N_i represents the number of unknowns in the extended block i; $\mathbf{E}_{ii}^{N_{\text{pws}}}$ is an $N_i \times N_{\text{pws}}$ excitation matrix; and $\mathbf{J}_{ii}^{\text{CBF}}$ is the PCBFs matrix of dimensions $N_i \times N_{\text{pws}}$. The PCBFs of block i can be obtained by directly solving (1). In order to improve the accuracy at the lower frequency points, the SCBFs are constructed by using the Foldy-Lax equations theory [12, 15]. The SCBFs $\mathbf{J}_i^{S1}$ and $\mathbf{J}_i^{S2}$ of block i are calculated by

$$\begin{aligned} \mathbf{Z}_{ii}\mathbf{J}_i^{S1} &= -\sum_{j=1(j\neq i)}^{M} \mathbf{Z}_{ij}\mathbf{J}_j^{P}, \\ \mathbf{Z}_{ii}\mathbf{J}_i^{S2} &= -\sum_{j=1(j\neq i)}^{M} \mathbf{Z}_{ij}\mathbf{J}_j^{S1}, \end{aligned} \tag{2}$$

where $\mathbf{Z}_{ij}$ is the impedance matrix of block i and block j. Following the above described procedure, $2N_\theta N_\phi \mathbf{J}^P$, $2N_\theta N_\phi \mathbf{J}^{S1}$, and $2N_\theta N_\phi \mathbf{J}^{S2}$ can be obtained. Typically, the number of PWs that have been used to generate the CBFs would exceed the number of degrees of freedom associated with the block and, therefore, it is desirable to use the SVD procedure to remove the redundancy in these CBFs. Only the relative singular values above a certain threshold, for example, $1.0E-3$, are retained as the IUCBFs. Assuming that there are K IUCBFs retained on each block after SVD, the surface current can be expressed as a linear combination of the IUCBFs as follows:

$$\mathbf{J} = \sum_{m=1}^{M}\sum_{k=1}^{K} \alpha_m^k J_m^{\text{CBF}_k}, \tag{3}$$

where $J_m^{\text{CBF}_k}$ represents the kth IUCBFs of block m and α_m^k represents the unknown weight coefficients. Galerkin method is used to convert the traditional MoM equation into a linear equation about coefficient matrix $\boldsymbol{\alpha}$. A $KM \times KM$ reduced matrix can be obtained:

$$\mathbf{Z}^{\mathbf{R}} \cdot \boldsymbol{\alpha} = \mathbf{V}^{\mathbf{R}}, \tag{4}$$

where $\mathbf{V}_i^{\mathbf{R}} = \mathbf{J}^T \cdot \mathbf{E}_i$, T represents the transposition, and $\mathbf{Z}^{\mathbf{R}}$ represents the reduced impedance matrix of dimensions $KM \times KM$. Its detailed calculation expression can be expressed as follows:

$$Z_{ij}^R = \mathbf{J}^T \cdot \mathbf{Z}_{ij} \cdot \mathbf{J} \quad i, j \leq M, \tag{5}$$

where $\mathbf{Z}_{ij}$ represents the impedance matrix between i and j blocks. Typically, the dimensions of the reduced matrix $\mathbf{Z}^{\mathbf{R}}$ are smaller than that generated via the conventional MoM, and $\boldsymbol{\alpha}$ can be obtained by directly solving (4). In this way, the surface current at any frequency point can be obtained. Although the IUCBFs can improve the calculation accuracy at lower frequency points, it should be noted that the increase in the size of the targets under analysis will increase the number of the PWs and the generating procedure for the PCBFs in IUCBFM will still require expensive time. It is desirable to speed up the PCBFs generation by reducing the number of the PWs.

3. SVD Enhanced CBFs Generation

In order to obtain enough CBFs for a given SVD threshold and for arbitrary geometries in the blocks, the redundant

Table 1: Number of PWs and IUCBFs and computational time of the sphere.

	IUCBFM			SVD-IUCBFM		
Frequency subband (GHz)	0.2–0.65	0.65–1.1	1.1–2.0	0.2–0.65	0.65–1.1	1.1–2.0
Number of PWs	128	128	128	23	33	54
SVD time (s)	9.55	9.03	8.25	5.61	6.09	8.29
Number of IUCBFs	344	551	809	316	517	706
IUCBFs construction time (s)	216.54	213.27	207.21	98.94	111.94	152.79
Reduced matrix filling (s)	108.27	279.17	564.01	87.56	207.21	418.26
Total time (s)	2135.25	4159.47	7016.52	1919.54	3336.54	5365.49

PWs are usually chosen [11–14]. However, the redundancy of the PWs increases the solving time of the CBFs. To mitigate this problem, the SVD procedure is adapted to enhance the efficiency of the CBFs generation in this paper.

As done in [12], each block is irradiated with multiangle PWs and an excitation matrix $\mathbf{E}_{ii}^{N_{\text{pws}}}$ is obtained with size $N_i \times N_{\text{pws}}$. Typically, the number of PWs that have been used to generate the CBFs would exceed the number of degrees of freedom associated with the block, so the excitation matrix would contain linear dependencies and can be compressed to remove the redundancy in the incident field. In this paper, the SVD procedure is applied to remove the redundancy in the excitation matrix. This is done by expressing this latter as

$$\mathbf{E}_{ii}^{N_{\text{pws}}} = \mathbf{U}\mathbf{D}\mathbf{V}^T, \tag{6}$$

where $\mathbf{U}$ is an $N_i \times N_i$ orthogonal matrix, $\mathbf{V}^T$ is an $N_{\text{pws}} \times N_{\text{pws}}$ orthogonal matrix, and $\mathbf{D}$ is an $N_i \times N_{\text{pws}}$ diagonal matrix. The superscript T denotes the transpose operation. The authors retain the columns from the left singular value matrix $\mathbf{U}$ whose singular values are above a threshold ε, typically chosen to be $1.0E-3$. Thus, a new excitation matrix named $\mathbf{E}_{ii}^{\text{New}}$ is obtained and the number of incident PWs is decreased. For simplicity, suppose there are L incident PWs for each block after the SVD and the dimensions of $\mathbf{E}_{ii}^{\text{New}}$ are $N_i \times L$, where L is always smaller than N_{pws}. After $\mathbf{E}_{ii}^{N_{\text{pws}}}$ is replaced by $\mathbf{E}_{ii}^{\text{New}}$ in (1), the PCBFs $\mathbf{J}_i^P$ of block i can be obtained by solving the following linear system of equations:

$$\mathbf{Z}_{ii} \cdot \mathbf{J}_{ii}^{\text{CBF}} = \mathbf{E}_{ii}^{\text{New}}. \tag{7}$$

Once the PCBFs of each block are solved, the generation of the SCBFs is the same as described in [12]. The total number of matrix equation solutions required to generate the CBFs is $3M \cdot L$, which is smaller than $3M \cdot N_{\text{pws}}$ in the IUCBFM as $L \ll N_{\text{pws}}$. Following the above described procedure, $3L$ CBFs will exist for each block (including L PCBFs and $2L$ SCBFs). Once again, the SVD procedure is used to further reduce the linear dependency among these CBFs. For simplicity, it is assumed that all of the blocks contain the same number L_{New} of IUCBFs. The dimensions of the reduced matrix will be reduced to $ML_{\text{New}} \times ML_{\text{New}}$, which is a significant reduction compared to $MK \times MK$ in the IUCBFM as $L_{\text{New}} \ll K$.

4. Numerical Results

In order to validate the accuracy and efficiency of the proposed approach, several numerical examples are presented for the scattering from PEC objects. All the computations are carried out on a personal computer with a 3.0 GHz Intel(R) Pentium(R) G2030 CPU and 4 GB RAM (only one core is used). The second level of the SCBFs is calculated. In the conventional IUCBFM, the threshold of the SVD for generating the CBFs is $1.0E-3$. In the proposed method (SVD-IUCBFM), the thresholds of the SVD for compressing the PWs and generating the CBFs are set to $1.0E-3$ and $1.0E-2$, respectively. In order to decrease the computational complexity at the lower frequency points, the adaptive IUCBFs construction method is used [13].

First, the scattering problem of a PEC sphere with radius of 0.1 m is considered over a frequency range of 0.2 to 2 GHz. The object is divided into 2200 triangular patches with an average length of $\lambda/10$ at 2 GHz and the total number of unknowns is 5790. Referring to [12], each block is illuminated by multiangle PWs from $0^\circ \le \theta < 180^\circ$ and $0^\circ \le \varphi < 360^\circ$ with $N_\theta = 8$ and $N_\phi = 8$, which results in a total of 384 PWs. In the SVD-IUCBFM, 8 PWs in directions of θ and ϕ are set. After SVD, only 37 new excitation vectors (average value) relative to the largest singular value are retained on each block which results in a new excitation matrix $\mathbf{E}_{ii}^{\text{New}}$. Compared with the IUCBFM, the dimensions of excitation matrix are dramatically reduced. By exciting each block with new excitation matrix and solving the linear system of equations, $37\mathbf{J}^P$, $37\mathbf{J}^{S1}$, and $37\mathbf{J}^{S2}$can be obtained on each block. The SVD is again used to further reduce the linear dependency among these CBFs. The number of the IUCBFs retained on each block and the SVD time of two methods in each subband are given in Table 1 in detail. It can easily be observed that the number of the IUCBFs obtained using the SVD-IUCBFM is evidently smaller than that obtained using the IUCBFM and the time of SVD is reduced because of the reduced CBFs matrix dimensions. The bistatic RCS in $\theta\theta$ polarization calculated by the IUCBFM, the MoM (FEKO),

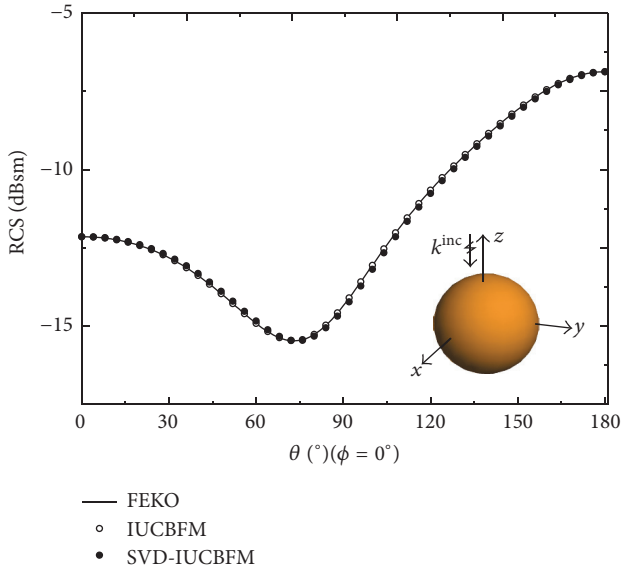

Figure 1: Bistatic RCS of the sphere at 1100 MHz.

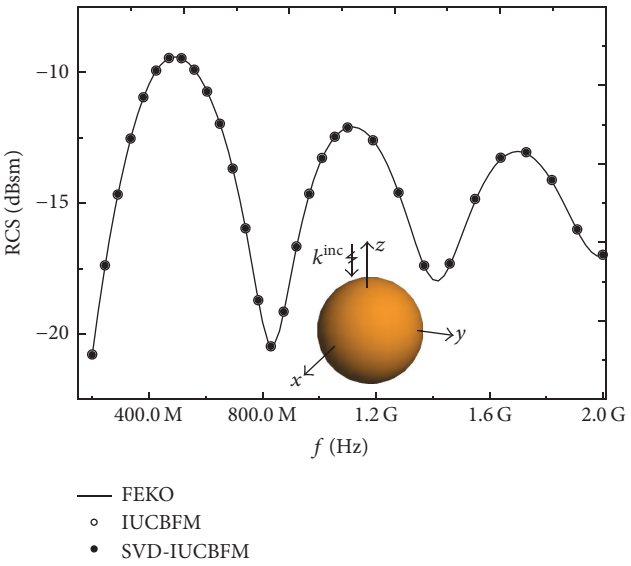

Figure 2: Broadband RCS of the sphere.

and the SVD-IUCBFM at 1100 MHz are shown in Figure 1. It can be seen that the SVD-IUCBFM shows an excellent agreement with the MoM. The broadband RCS (10 frequency sampling points in each subband) are obtained by using the IUCBFM and the SVD-IUCBFM over a frequency range of 0.2 to 2 GHz, as shown in Figure 2. The results calculated by using the SVD-IUCBFM agree well with the results obtained by the IUCBFM. Table 1 lists the numbers of the PWs and the IUCBFs and the computational time of the two methods. It can be seen that the SVD-IUCBFM reduced the PWs by using the SVD compared with the IUCBFM. Furthermore, the efficiencies of generating the CBFs and constructing the reduced matrix are both improved.

Second, a PEC cylinder over a frequency range of 0.1 to 2 GHz is considered. The radius and height of the cylinder are

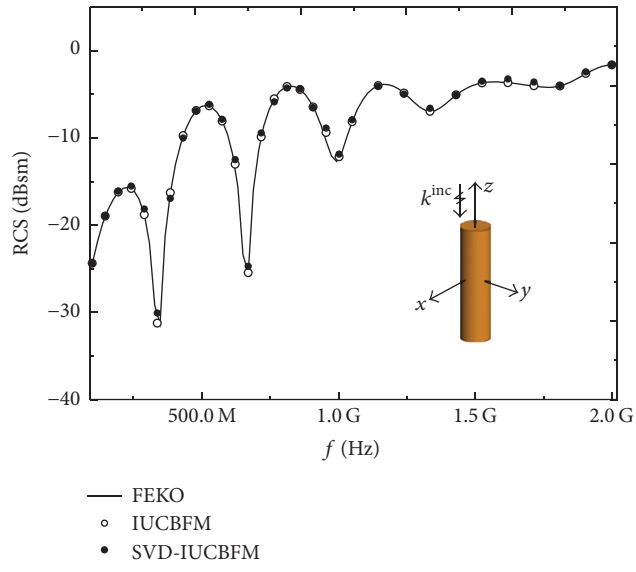

Figure 3: Broadband RCS of the cylinder.

0.1 m and 0.4 m, respectively. The object is divided into 5674 triangular patches and the number of unknowns is 12363. The cylinder is divided into 6 blocks. The broadband RCS (10 frequency sampling points in each subband) computed by the conventional IUCBFM and the SVD-IUCBFM are compared in Figure 3. Table 2 summarizes the numbers of the PWs and the IUCBFs and the computational time of the cylinder. It can be seen that the SVD-IUCBFM outperforms the conventional IUCBFM, both in CBFs generation and in RCS computational time. Particularly, the number of the PWs and the reduced matrix filling time are remarkably reduced and the gains are about 58% and 25%, respectively.

Finally, a PEC cube with a side length of 0.1 m over a frequency range of 0.1 to 5 GHz is considered. The discretization in triangular patches is conducted at 5 GHz which leads to a number of 13607 unknowns. The geometry is divided into 8 blocks. The broadband RCS computed by the IUCBFM and the SVD-IUCBFM are shown in Figure 4. A good agreement can be seen from the figure. The number of the PWs and the IUCBFs and the computational time are shown in Table 3. It can be seen that the SVD-IUCBFM need a smaller number of PWs by using the SVD procedure compared with the conventional IUCBFM. Furthermore, the reduced matrix dimensions and the reduced matrix filling time are both reduced.

5. Conclusion

In this paper, a new approach has been proposed to efficiently compute the wideband RCS of the PEC objects. In the proposed approach, the number of required PWs has been remarkably reduced by further compressing the incident PWs using the SVD, which results in fewer matrix equation solutions and decreases time of CBFs generation. Furthermore, the dimensions of the reduced matrix and the RCS computation time are both reduced compared with the

Table 2: Number of PWs and IUCBFs and computational time of the cylinder.

	IUCBFM			SVD-IUCBFM		
Frequency subband (GHz)	0.1–0.575	0.575–1.05	1.05–2.0	0.1–0.575	0.575–1.05	1.05–2.0
Number of PWs	128	128	128	31	48	81
SVD time (s)	82.70	79.27	79.29	65.66	77.32	81.86
Number of IUCBFs	402	649	1044	334	549	951
IUCBFs construction time (s)	1318.23	1315.72	1311.26	875.08	1012.41	1252.8
Reduced matrix filling (s)	5684.77	9976.09	15501.19	4293.39	7150.81	12070.43
RCS calculation time (s)	63203.93	102016.86	161399.16	48847.90	77564.81	125723.17

Table 3: Number of PWs and IUCBFs and computational time of the cylinder.

	IUCBFM				SVD-IUCBFM			
Frequency subband (GHz)	0.1–0.7125	0.7125–1.325	1.325–2.55	2.55–5.0	0.1–0.7125	0.7125–1.325	1.325–2.55	2.55–5.0
Number of PWs	128	128	128	128	20	24	41	73
SVD time (s)	50.37	50.55	51.09	51.69	30.91	32.73	43.21	73.27
Number of IUCBFs	365	476	728	1341	247	355	617	1191
IUCBFs construction time (s)	1421.12	1430.03	1428.43	1436.81	555.94	612.81	820.01	1072.36
Reduced matrix filling (s)	3416.11	5895.31	9772.54	19744.71	2324.82	5747.99	8591.35	14608.87
RCS calculation time (s)	41810.12	66620.11	105411.94	205182.12	29994.712	48222.06	92996.69	153532.42

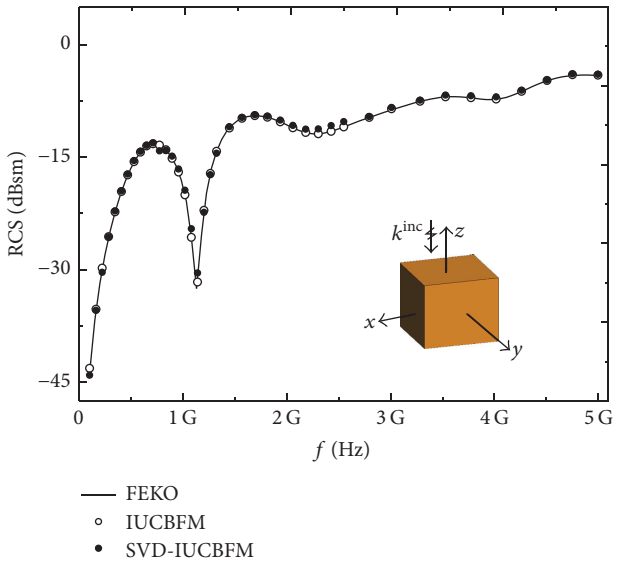

Figure 4: Broadband RCS of the cube.

traditional IUCBFM. The results have demonstrated that the proposed SVD-IUCBFM is able to more efficiently calculate the wideband RCS compared with the conventional IUCBFM without compromising the accuracy.

Competing Interests

The authors declare that they have no competing interests.

Acknowledgments

This work was supported by the National Natural Science Foundation of China under Grant no. 61401003, the Natural Science Foundation of Anhui Provincial Education Department under Grant no. KJ2016A669, and the Natural Science Foundation of Huainan Normal University under Grant no. 2015xj09zd.

References

[1] R. F. Harrington, *Field Computation by Method of Moments*, IEEE Press, New York, NY, USA, 1992.

[2] R. Coifman, V. Rokhlin, and S. Wandzura, "The fast multipole method for the wave equation: a pedestrian prescription," *IEEE Antennas and Propagation Magazine*, vol. 35, no. 3, pp. 7–12, 1993.

[3] J. Song, C.-C. Lu, and W. C. Chew, "Multilevel fast multipole algorithm for electromagnetic scattering by large complex objects," *IEEE Transactions on Antennas and Propagation*, vol. 45, no. 10, pp. 1488–1493, 1997.

[4] M. Chen, R. S. Chen, and X. Q. Hu, "Augmented MLFMM for analysis of scattering from PEC object with fine structures,"

Applied Computational Electromagnetics Society Journal, vol. 26, no. 5, pp. 418–428, 2011.

[5] E. Bleszynski, M. Bleszynski, and T. Jaroszewicz, "AIM: adaptive integral method for solving large-scale electromagnetic scattering and radiation problems," *Radio Science*, vol. 31, no. 5, pp. 1225–1251, 1996.

[6] K. Zhao, M. N. Vouvakis, and J.-F. Lee, "The adaptive cross approximation algorithm for accelerated method of moments computations of EMC problems," *IEEE Transactions on Electromagnetic Compatibility*, vol. 47, no. 4, pp. 763–773, 2005.

[7] V. V. S. Prakash and R. Mittra, "Characteristic basis function method: a new technique for efficient solution of method of moments matrix equations," *Microwave and Optical Technology Letters*, vol. 36, no. 2, pp. 95–100, 2003.

[8] E. Lucente, A. Monorchio, and R. Mittra, "An iteration-free MoM approach based on excitation independent characteristic basis functions for solving large multiscale electromagnetic scattering problems," *IEEE Transactions on Antennas and Propagation*, vol. 56, no. 4, pp. 999–1007, 2008.

[9] E. H. Newman, "Generation of wide-band data from the method of moments by interpolating the impedance matrix (EM problems)," *IEEE Transactions on Antennas and Propagation*, vol. 36, no. 12, pp. 1820–1824, 1988.

[10] G. J. Burke, E. K. Miller, S. Chakrabarti, and K. Demarest, "Using model-based parameter estimation to increase the efficiency of computing electromagnetic transfer functions," *IEEE Transactions on Magnetics*, vol. 25, no. 4, pp. 2807–2809, 1989.

[11] M. De Gregorio, G. Tiberi, A. Monorchio, and R. Mittra, "Solution of wide band scattering problems using the characteristic basis function method," *IET Microwaves, Antennas and Propagation*, vol. 6, no. 1, pp. 60–66, 2012.

[12] W.-Y. Nie and Z.-G. Wang, "Solution for wide band scattering problems by using the improved ultra-wide band characteristic basis function method," *Progress in Electromagnetics Research Letters*, vol. 58, pp. 37–43, 2016.

[13] W. Y. Nie and Z. G. Wang, "Analysis of wide band scattering from objects using the adaptive improved ultra-wide band characteristic basis functions," *Progress in Electromagnetics Research Letters*, vol. 60, pp. 45–51, 2016.

[14] S. N. Koç and A. Köksal, "Wideband analysis of planar scalable antennas and PEC bodies using CBFM," *Turkish Journal of Electrical Engineering & Computer Sciences*, vol. 24, pp. 1652–1662, 2016.

[15] Z. G. Wang, Y. F. Sun, and G. H. Wang, "Analysis of electromagnetic scattering from perfect electric conducting targets using improved characteristic basis function method and fast dipole method," *Journal of Electromagnetic Waves and Applications*, vol. 28, no. 7, pp. 893–902, 2014.